Cyclic deformation of TiAl generic microstructures at room and high temperature: Bauschinger effect & strain rate sensitivity

Pierre Serrano, Louise Toualbi, Pascale Kanoute, Alain Couret

Cyclic deformation of TiAl generic microstructures at room and high temperature: Bauschinger effect & strain rate sensitivity.

P. Serrano[a,*], L. Toualbi[a], P. Kanoute[a], A. Couret[b]

[a] *Onera - The French Aerospace Lab, Département Matériaux et Structures, F-92322 Châtillon, France*

[b] *CNRS, CEMES (Centre d'Elaboration de Matériaux et d'Etudes Structurales), BP 94347, 29 rue J. Marvig, F-31055 Toulouse, France*

Abstract

The cyclic deformation of four TiAl common microstructures is studied experimentally at room and high temperature. Multilevel and multirate tests are performed to highlight the microstructure impact on the Bauschinger effect and the strain rate sensitivity. The mechanical behaviors are linked to their corresponding deformation mechanisms. Results can directly be used to develop microstructure-sensitive modeling of the mechanical behaviors of TiAl alloys.

Keywords: A. Intermetallics (aluminides), B. Cyclic plasticity, B. Plastic deformation mechanisms, D. Microstructure, E. Yield behavior, F. Mechanical testing

*Corresponding author

Email address: pierre.serrano@onera.fr (P. Serrano)

1. Introduction

Technological advances in aircraft engine design require the use of lightweight materials at increasingly high temperatures. Therefore, intermetallics titanium aluminide alloys based on γ-TiAl have been introduced in the most recent civil turbo-engines as low pressure turbine blades [1]. To extend the use of this material to other application technologies, new alloys are being developed with enhanced mechanical properties [2].

Recently, it has been shown that a significant Bauschinger effect occurs at room temperature on TiAl alloy upon strain reversal loading [3]. Even if this effect has been mentioned in some works [4, 5], few hysteresis loops analysis are available. It can even be stated that the link between the microstructure and the mechanical behavior is mostly understood upon uniaxial and monotonic loadings [6, 7, 8, 9].

Indeed, the thermomechanical behavior of TiAl alloys has been studied only on already optimized microstructures with balanced properties [10, 11, 12]. In [13], a comparison is made between a near-γ microstructure and a lamellar microstructure but tests are only performed at room temperature. Other works discuss the cyclic behavior but only by means of the stress or strain amplitude evolution [14, 5, 15, 16, 17]. On cited works, the Bauschinger effect is not studied.

Hysteresis loop analysis give additional information on the link between the macroscopic behavior and microstructural mechanisms [18]. Moreover, such results are extremely valuable to develop refined plasticity theory [19, 20]. In order to develop models that are able to describe the material behavior under the conditions seen by low pressure turbine blade, the cyclic behavior

must be known over a range of various strain ranges and strain rates [21]. To that attend, it has been shown that only a single multilevel and multirate cyclic test can be used [22].

The aim of this work is to study the link between TiAl microstructures and their corresponding mechanical behavior. The four generic microstructures of TiAl alloys are studied to correlate the macroscopic behavior to the corresponding microstructural mechanisms. Emphasis is made on the Bauschinger effect, but strain rate sensitivity is also considered so that the results can directly be used to develop advanced microstructure-sensitive models.

2. Material and methods

2.1. Microstructures

The material used is the G4 alloy (Ti-47Al-1Re-1W-0.2Si (at.%)) developed at the Onera and obtained via the powder metallurgy route [23]. The ingots have been casted at Howmet Casting facilities and the powder produced by argon gas atomization at Crucible Industries. Hot Isostatic Pressing (HIP) was performed by Bodycote at 140 MPa for 4h at 1250 °C. The chemical analysis of the powder compacts is given in Table 1.

Ti (at. %)	Al (at. %)	Re (at. %)	W (at. %)	Si (at. %)	C (ppm)	O (ppm)
50.85	47.01	0.95	0.95	0.24	175	1240

Table 1. Chemical composition of the studied G4 alloy.

Cylindrical blank were machined from the powder compacts. Heat treatments were directly applied on those specimens to control the microstructure.

Temperature induced porosity (TIP) is observed after the treatments because of gas entrapped inside the powder after the atomization. The same observations as in [24] were made : the occurence of TIP after temperature annealing depends on the grain size and the annealing time. TIP reduces drastically fatigue lifetime. However, in our case they have no impact on the macroscopic mechanical behavior and the hysteresis loop shape because of their low volume fraction (< 1 % for all microstructures) [25].

For microscopic observations, samples were ground with a series of emery papers, then polished with colloidal silica paste abrasives down to 0.25 µm. Microstructures were examined with a scanning electron microscope (SEM) by back scattered electron images (BSE). Microstructural parameters were quantified by image segmentation using ImageJ, a Java-based image processing program [26]. The apparent surface of grains was measured. The grain size is taken as the equivalent diameter of the measured shape. Series of micrographs were examined to ensure that the observations were statistically representatives. The lamellae spacing was measured following the methodology proposed in [27] for two types of cooling heat treatments: furnace and air cooling. The sample was cut in half and the apparent lamellar spacing and angle were measured on both side after polishing. A stereological correction is then applied to access the real lamellar spacing. Again, series of measurements were made to ensure that the observations were statistically representatives.

SEM images of the studied microstructures are shown in Fig. 1. The post-HIP microstructure is a near-γ microstructure (Fig. 1a) that contains mainly small equiaxed γ grains with a mean size of 5 µm. Smaller β_0 ($\sim$ 2.5 %) and α_2 ($\sim$ 2.5 %) equiaxed grains are also observed with a mean size

	γ		α_2		β_0		$\alpha_2+\gamma$		
	VF (%)	GS (µm)	VF (%)	GS (µm)	VF (%)	GS (µm)	VF (%)	GS (µm)	LS (µm)
Near-γ	95	5	2.5	2	2.5	2	-	-	-
Duplex	50	8	-	-	-	-	50	15	0.08
Near-lamellar	10	8	-	-	-	-	90	50	0.08
Lamellar	-	-	-	-	-	-	100	200	0.3

Table 2. Results of the microstructural characterization. VF stands for Volume Fraction, GS stands for Grain Size, LS stands for Lamellae Size.

of 2 µm.

The duplex microstructure (Fig. 1b) is obtained following a heat treatment at 1340 °C during 4 hours followed by an air cooling. This microstructure contains equiaxed γ grains ($\sim$ 5 µm) and lamellar colonies ($\sim$ 15 µm). The grains are surrounded by borders consisting of γ phase and β_0 precipitates as observed in the IRIS alloy [28].

The near-lamellar microstructure (Fig. 1c) is obtained following a heat treatment at 1360 °C during 1 hour followed by an air cooling. This microstructure contains mainly relatively small lamellar colonies ($\sim$ 90 %, $\sim$ 50 μm). Some equiaxed γ grains ($\sim$ 10 %, $\sim$ 8 μm) are still present. All phases are surrounded by borders again.

Finally, the lamellar microstructure (Fig. 1d) is obtained following a heat treatment at 1370 °C during 1 hour with a furnace cooling. This microstructure contains large lamellar grains ($\sim$ 200 μm) surrounded by the border phase. The results of the microstructural characterization are given in Table 2.

It has to be noticed that getting accurate measurements of the TiAl

microstructural attributes is difficult even by Electron BackScatter Diffraction (EBSD) because of the lamellae size and the pseudo-symmetry of the γ-phase. For our case, statistical measurement performed by hand was find to be the most relevant method.

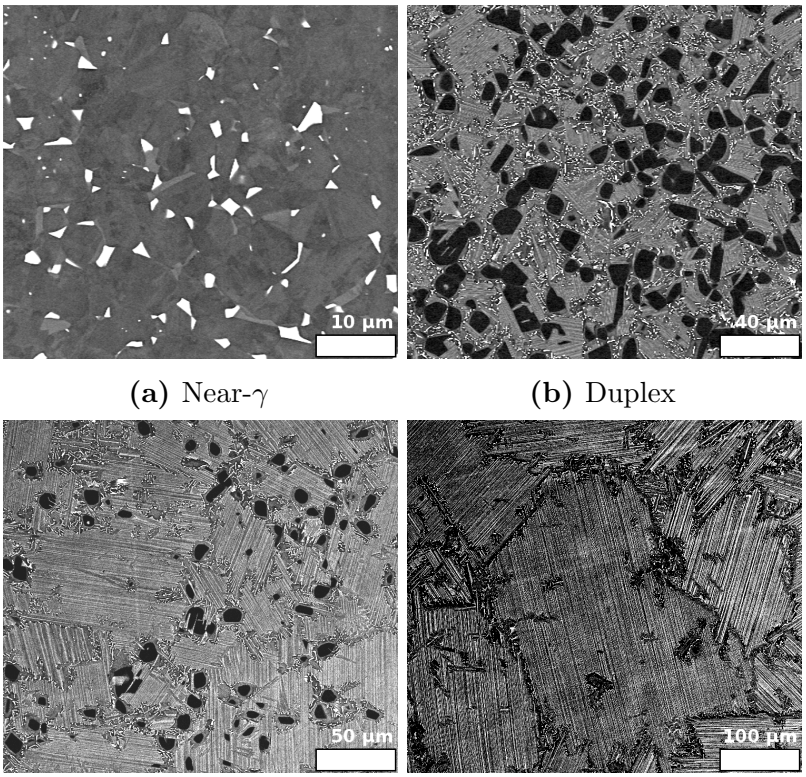

(a) Near-γ **(b)** Duplex

(c) Near-lamellar **(d)** Lamellar

Fig. 1. SEM micrographs of the generic microstructures studied in this work.

2.2. Mechanical testing

For mechanical testing, cylindrical specimens were machined with the geometry specified in Fig. 2. As described in [14], the size of the gauge section was optimized to ensure that it contains at least 250 grains for every

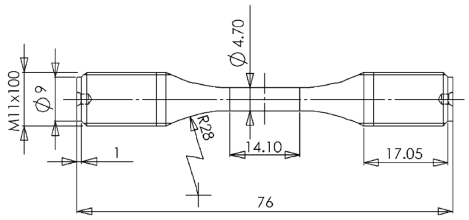

Fig. 2. Test specimen geometry.

investigated microstructure. Room temperature and high temperature tests at 750 °C were conducted in air atmosphere using a MTS servohydraulic machine. High temperature tests were performed using a furnace monitored by three thermocouples attached to the specimen. Extensometers attached directly to the gauge part of the specimens were used. Tests were performed in total mechanical strain control with a triangular waveform. Hence, the plastic strain rate is not constant [29]. Nevertheless, this is the case in various works in which both the Bauschinger effect and strain rate sensitivity were investigated [3, 18, 30]. As all the specimens undergo the same type of loading, we assume that it has a limited impact on the observed mechanical behaviors and the discussion [31].

At both room temperature and 750 °C, a tensile test was first performed. Results were used to determine appropriate strain range level for each microstructure and to compare monotonic and cyclic behaviors. The strain rate at room temperature is $\dot{\varepsilon} = 10^{-3}$ s^{-1}. At 750 °C, the viscous behavior was investigated by changing the strain rate to $\dot{\varepsilon} = 10^{-5}$ s^{-1} during the test, then by stopping the test at $\varepsilon = 0.8$ % and performing a 8 hours relaxation to study the mechanical behavior upon very low strain rate.

Multilevel cyclic tests were performed in symmetric tension-compression

cycle (R_ε = -1) at $\dot{\varepsilon} = 10^{-3}\ \mathrm{s}^{-1}$ for room temperature tests and multiple strain rates for high temperature tests. Strain range levels were defined based on tensile test results. This type of cyclic tests highlights the major characteristics of the mechanical behavior with a limited number of specimens and is suited to the development of refined plasticity theories.

2.3. Bauschinger effect analysis

The mechanical behavior of material upon strain reversal loading is usually characterized by the Bauschinger effect, defined as a reduction of the yield stress upon load reversal [32]. A scheme showing the typical stress-strain behavior under strain controlled symmetric tension-compression tests is shown in Fig. 3. Quantities detailed below are measured and used to discuss the microstructure influence on this effect.

For tensile test and the first cycle of cyclic tests, the yield stress σ_0 and 0.2 % yield stress $\sigma_{0.2}$ are respectively defined as the lowest stress point at which permanent deformation can be measured and the stress at 0.2 % plastic strain. A Bauschinger effect is observed if the compressive yield stress σ_c is lower than the yield stress such that $|\sigma_c| < |\sigma_0|$. This effect can be caused by different phenomena.

It has been stated that in the case of TiAl alloys, the Bauschinger effect is mainly caused by a significant transient softening [3]. This transient softening can be seen as a decrease of the initial elastic domain ED_0 defined as $ED_0 = 2\sigma_0$, that becomes ED_C upon load reversal [33, 34]. The transient softening can therefore be quantified as $TS_{OC} = ED_0 - ED_C$.

Even in the case where $ED_0 = ED_C$, a Bauschinger effect is still observed if there is kinematic hardening. This is defined as the displacement of the

initial elastic domain center, the point A on the scheme, that becomes point B upon load reversal. This leads once again to a lower compressive yield stress σ_c as $|\sigma_c| < |\sigma_0|$.

Cyclic plasticity experiments with R_ε = -1 can also reveal a tension-compression asymmetry [20]. Such asymmetry is usually discussed by studying the difference between the stress at the maximal peak strain σ_1 and the stress at the minimal peak strain, σ_2. Another interesting way to reveal a tension-compression asymmetry is to compare the size of the elastic domain upon compression, ED_C, to the size of the elastic domain upon tension, ED_T.

It should be noted that the Bauschinger effect can also be caused by a permanent softening, which is defined by a loss of strength between the forward and reverse parts of the test [35]. As it has already been shown that it does not happen in the case of TiAl alloys in [3], it will not be mentioned thereafter.

Finally, the evolution of the elastic domains, the peak stresses and the hysteresis loop shapes over the course of the test are studied to get insight over a potential cyclic hardening or softening.

The size of the elastic domain is measured on the stabilized hysteresis loops by using Cottrell's method [36]. This method has been widely used and discussed elsewhere [18, 37, 38, 39, 40]. It consists in extracting the elastic part of the hysteresis loop by considering that it corresponds to all the data points located between two parallel lines. Those lines have a slope equal to Young's modulus and are shifted by a strain offset. This offset parameter is defined based on the sensitivity of the extensometer. In our case, we use $\varepsilon_{\text{offset}} = (3 \pm 2) \times 10^{-5}$ as in [41]. A scheme illustrating the technique is shown

on the right part of Fig. 3. In some cases, the elasticity modulus can change during the test and has to be adjusted for the elastic part detection [42]. This was not necessary in our study.

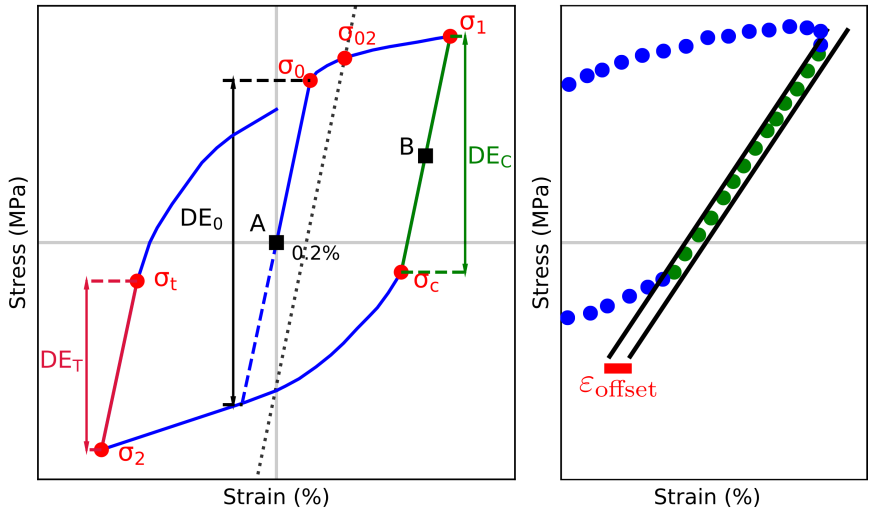

Fig. 3. Cyclic stress-strain behavior scheme. σ_0 is the yield stress, σ_{02} the 0.2% yield stress, σ_1 and σ_2 are the stresses respectively at the maximum and minimum peak strain, σ_C and σ_T are respectively the compressive and tensile yield strength during a fully reversed cycle. ED_0, ED_C and ED_T are respectively, the initial elastic domain, the compressive elastic domain and the tensile elastic domain. Points A and B are the centers of their corresponding elastic domains. The right part of the scheme illustrates the detection technique of the linear part based on the use of an offset parameter $\varepsilon_{\text{offset}}$.

3. Results

3.1. Room temperature tests

Room temperature tensile properties are illustrated in Fig. 4. The ductility is limited regardless of the microstructure. The microstructures exhibit various

behavior. The near-γ shows the highest stress state with an initial bump. The duplex microstructure shows a steep entry in plasticity and linear hardening. For the near-lamellar and the lamellar microstructure the elastic-plastic transition is smoother. Their yield stresses are equals, but differences in hardening led to different $\sigma_{0.2\%}$.

Multilevel cycle tests were designed to study the elastic-plastic transition by performing 5 cycles at $\Delta\varepsilon = 0.1$ %, 5 cycles at $\Delta\varepsilon = 0.2$ % and cycles up to specimen failure at $\Delta\varepsilon = 0.4$ %. Results are shown in Fig. 5. Poor powder quality induced failure after a small number of cycles, but enough were performed to analyze the cyclic stress strain behavior.

For all microstructures, the mechanical behavior during the first strain range level is elastic as no permanent strain is observed and σ_0 is not reached. The initial elastic domain is therefore clearly defined by $ED_0 = 2\sigma_0$. Then, a typical Bauschinger effect is observed for all microstructure after the onset of plasticity. This effect is mainly caused by a significant transient softening (i.e. ED_0 is reduced to ED_C and ED_T (see section 2.3)) but a kinematic hardening is also observed. The stabilized hysteresis loop is immediately reached as only the level transition cycles (dashed lines on the figures) are different from the others. Almost no cyclic hardening or softening are observed for all microstructures and there is no modification of the loop shapes until failure. When comparing the near-lamellar and lamellar microstructures, it can observed that plasticity starts in both cases at $\Delta\varepsilon/2 = 0.2$ % as the yield stress are the same, but that the hysteresis loop is more open for the lamellar microstructure.

To discuss the Bauschinger effect causes, the stress is plotted as a function

of the plastic strain for the stabilized hysteresis loops corresponding to $\Delta\varepsilon/2 = 0.4$ % in Fig. 6a. The kinematic hardening observed for the near-lamellar microstructure is more pronounced than the one of the lamellar microstructure. Indeed, for both microstructures, the initial elastic domains ED_0 and their associated centers are identical. But it can be observed in Fig. 6a that at $\Delta\varepsilon/2 = 0.4$ %, the elastic domain center of the near-lamellar microstructure is now at a higher position than the one of the lamellar microstructure.

The elastic domain sizes can be easily measured from those hysteresis loops, as they correspond to the stress range for which no plastic strain occurs. The elastic domain sizes upon compressive and tensile stress (ED_C and ED_T) are measured, and the transient softening is quantified as $TS_{OC} = ED_0 - ED_C$ and $TS_{OT} = ED_0 - ED_T$. The evolution of the elastic domains size and transient softening as a function of the γ phase volume fraction are shown in Fig. 6b.

The transient softening increases dramatically with the γ phase volume fraction. The comparison between the elastic domain sizes upon compressive and tensile stress reveals a pronounced tension-compression asymmetry for the two microstructures that contains a significant γ phase volume fraction. Regarding both lamellar microstructures, their elastic domain sizes and transient softenings are equals.

3.2. High temperature tests

Tensile tests at two strain rates followed by a 8 hours relaxation were performed at 750 °C. The results are shown in Fig. 7. The strain rate modification was made at $\varepsilon = 0.4$ % and $\varepsilon = 0.6$ % based on the results at

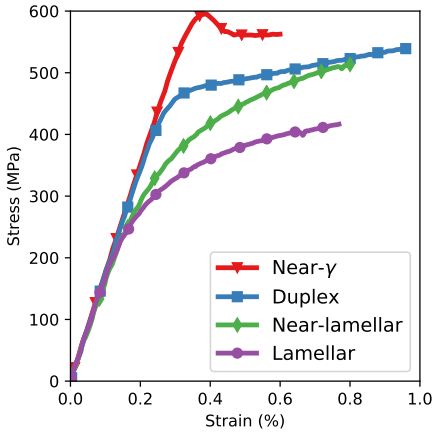

Fig. 4. Tensile curves at room temperature, $\dot{\varepsilon} = 10^{-3}$ s^{-1}.

room temperature to avoid early failure (see Fig. 7a).

The behavior is now ductile. A decrease of the mechanical properties (Young modulus, yield stresses) is observed compared to room temperature tests. Nevertheless, the microstructure strength hierarchy is the same, and the observations made regarding the plasticity and hardening behavior are still true. It is not possible to say if the bump on the near-γ microstructure has disappeared, as it might have occurred simultaneously with the first strain rate change.

The strain rate modification reveals the microstructure impact on the viscosity. The strain rate sensitivity is discussed through the stress gap that occurs during the strain rate modification. The near-γ microstructure presents the most viscosity effects, followed by the duplex. The near-lamellar and lamellar microstructures show almost no strain rate sensitivity. During the 8 hours relaxation, the mechanical behavior upon very low strain rate is revealed (Fig. 7b). The lamellar microstructure shows low relaxation whereas the near-lamellar has almost the same behavior as the duplex and near-γ

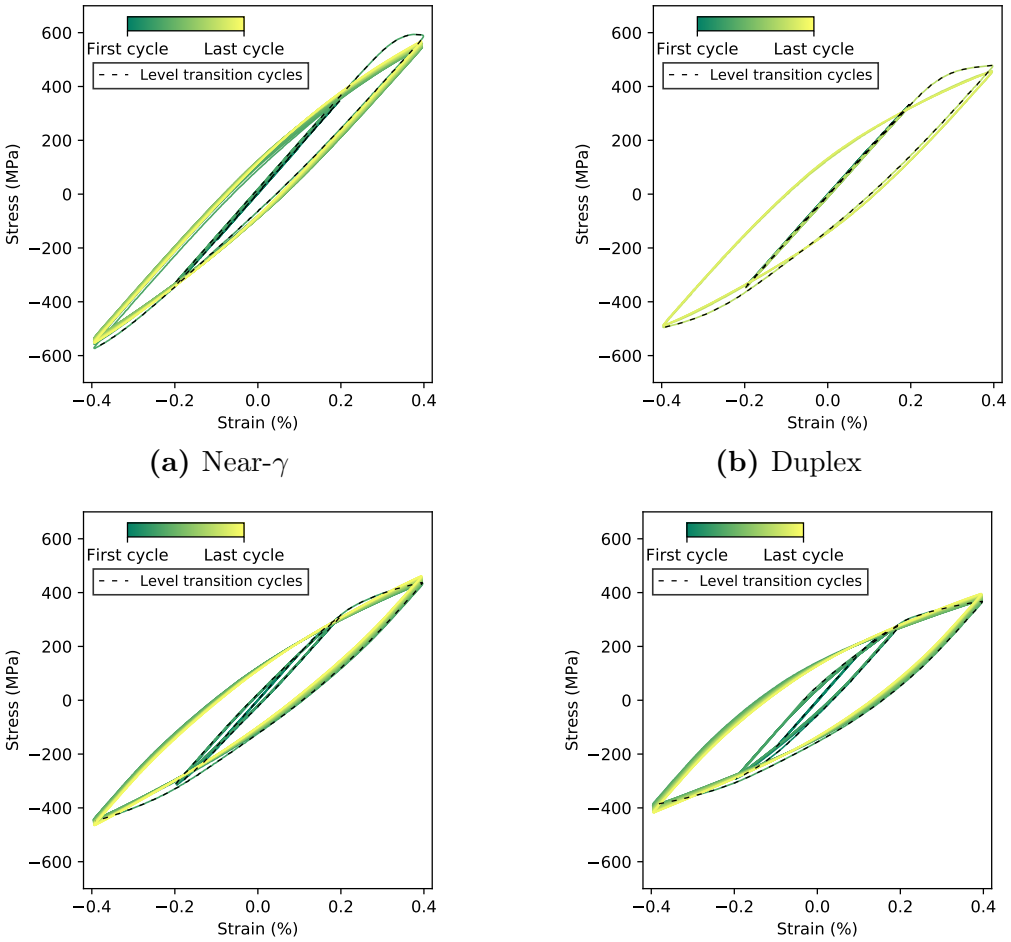

(a) Near-γ **(b)** Duplex

(c) Near-lamellar **(d)** Lamellar

Fig. 5. Room temperature multilevel cyclic tests results, $\dot{\varepsilon} = 10^{-3}\ \mathrm{s}^{-1}$.

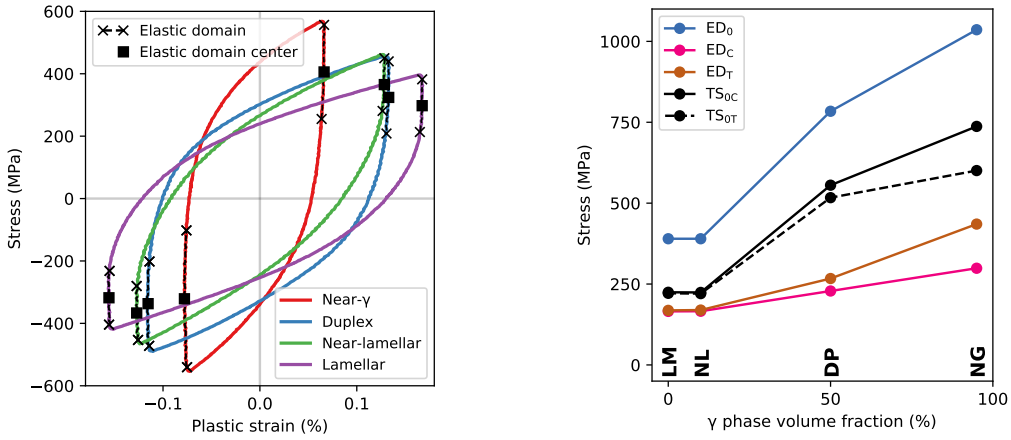

(a) Hysteresis loops for $\Delta\varepsilon = 0.4$ %. **(b)** Elastic domain evolution.

Fig. 6. Bauschinger effect analysis at room temperature. NG, DP, NL and LM respectively stand for Near-γ, Duplex, Near-lamellar and Lamellar microstructure. (For interpretation of the references to color in this figure legend, the reader is referred to the Web version of this article.)

microstructure. Therefore, a small amount of globular γ phase on a TiAl microstructure significantly modifies the low strain rate mechanical behavior.

Multilevel and multistrain cyclic tests are conducted in tension-compression under strain controlled at 750 °C. At each strain amplitude, 64 cycles are performed at a strain rate $\dot{\varepsilon} = 10^{-3}$ s^{-1}, 32 at $\dot{\varepsilon} = 10^{-4}$ s^{-1} and 8 at $\dot{\varepsilon} = 10^{-5}$ s^{-1}. Successive strain amplitudes were defined to get enough data from each microstructure based on their room temperature and high temperature tensile test results to avoid early failure. The amplitudes are 0.4 %, 0.6 %, 0.8 % and 1 % for the near-γ and duplex microstructures. The amplitudes are 0.2 %, 0.4 %, 0.6 % and 0.8 % for the near-lamellar and lamellar microstructures. Results are shown in Fig. 8.

Once again, stabilized cycle is reached immediately and the strain rate

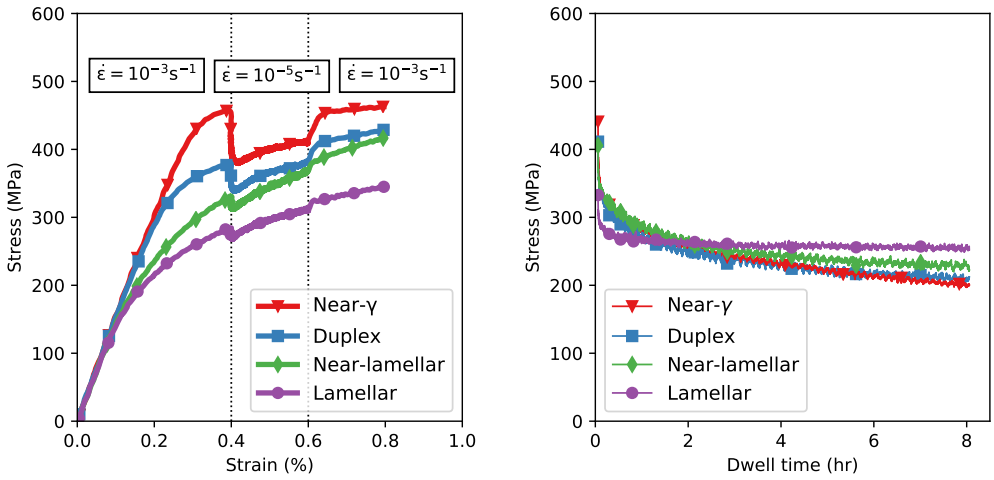

Fig. 7. High temperature tensile tests at two strain rates (a) follow by an 8 hours relaxation (b).

sensitivity increases with increasing γ phase volume fraction. For the near-γ microstructure, an important initial transient softening is observed. This might indicate that the mechanisms responsible for the bump at room temperature are still activated at 750 °C as shown by the zoom in Fig. 8a. No cyclic hardening or softening was observed regardless of the microstructure.

As for the room temperature results, the stress as a function of the plastic strain for the stabilized $\Delta\varepsilon/2 = 0.6$ % hysteresis loops and the evolution of the elastic domain sizes are studied. The results are shown in Fig. 9a and Fig. 9b. Remarkably, the transient softening observed for each microstructure is almost the same at 750 °C than the one observed at room temperature. Finally, the tension-compression asymmetry of the near-γ microstructure has decreased and is almost insignificant.

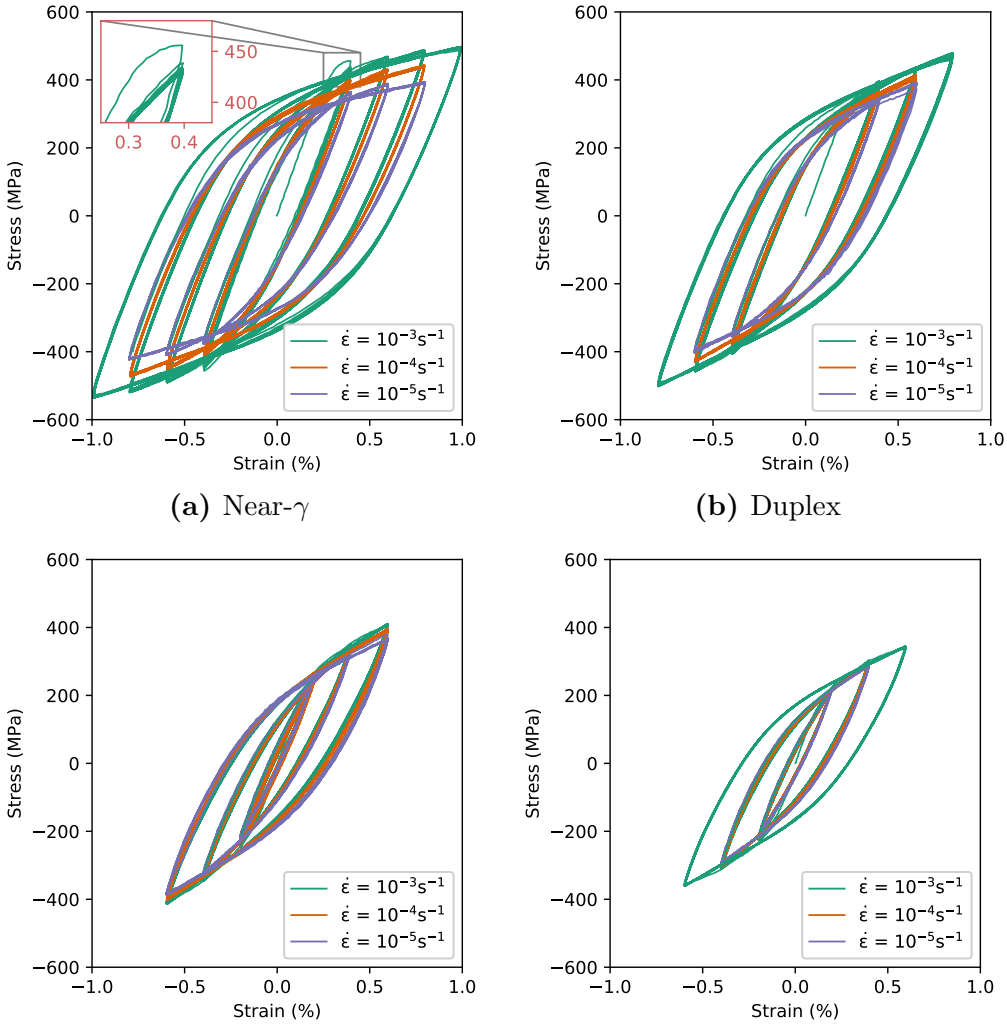

(a) Near-γ **(b)** Duplex

(c) Near-lamellar **(d)** Lamellar

Fig. 8. Multilevel and multirate cyclic tests at 750 °C results. (For interpretation of the references to color in this figure legend, the reader is referred to the Web version of this article.)

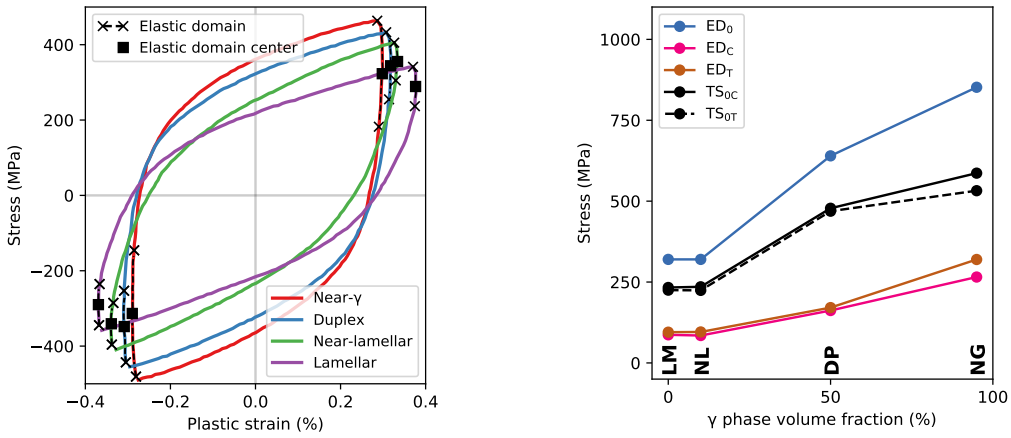

(a) Hysteresis loops for $\Delta\varepsilon = 0.6$ %. **(b)** Elastic domain evolution.

Fig. 9. Bauschinger effect analysis at 750 °C. NG, DP, NL and LM respectively stand for Near-γ, Duplex, Near-lamellar and Lamellar microstructure. (For interpretation of the references to color in this figure legend, the reader is referred to the Web version of this article.)

4. Discussion

The microstructure strength hierarchy observed here is similar to the one commonly observed at room temperature in the literature [6, 43]. A classical Hall-Petch relationship between yield stress and the grain/colony size is followed as observed elsewhere [44]. Indeed, even if in the case of the fully lamellar microstructure the lamellae thickness is sub-micrometric, once the soft colonies are deformed the mean free path of the dislocation within the lamellae habit plane is very important because of the lamellar colony size. We also point out that the lamellae width affects the yield strength for microstructures with similar colony size [45].

At room temperature and 750 °C and for strain rate in the range from

10^{-3} s^{-1} to 10^{-5} s^{-1}, plastic deformation in TiAl occurs by glide of ordinary dislocations and twinning [7, 46]. At 750 °C, the deformation is eased by the activation of cross slip. Superdislocations are generally reported as a deformation mechanism for the γ phase. However, as they are almost never observed experimentally in conventional alloys and in the investigated alloy their contribution to the deformation is supposed very small [47, 48]. Therefore, they are not considered in the following discussion. Based on the experimental results, the mechanical behavior of TiAl microstructures can be classified in two categories.

The first type of behavior corresponds to microstrutures with a high γ phase volume fraction, in our case the near-γ and duplex. Their behavior is characterized by a steep entry into plasticity, with an initial bump for the near γ microstructure, followed by a pronounced transient softening upon reverse flow stress. The bump phenomena was linked to the activation of the first twinning systems in [49, 50]. It might be related to the fact that twin nucleation is more difficult than twin propagation [51]. Detailed TEM and neutron diffraction investigations during cyclic tests suggest that major twins are nucleated when the strain range increase, i.e. during the first cycle of the considered strain range level [52]. This twin nucleation during the first loading part creates interfaces. TEM investigations of TiAl deformation and dislocation dynamic simulations confirmed that those boundaries are obstacles to dislocation movement, and therefore back stress generators [53, 54]. Furthermore, it was observed on steel that this back stress does create a significant Bauschinger effect caused by transient softening [55].

Based on the extensive microstructural analysis available in the literature,

the following scenario can be defined. Twins are created during the first loading part of cyclic tests, therefore creating new boundaries within grains and an important back stress when interacting with dislocations. Because the shortness of their Burgers vector and since only one twinning dislocation can propagate in each plane, twinning is able to bring only a moderate amount of strain. Hence, the subsequent strain is largely due to glide of ordinary dislocations, the movement of which being impacted by the twins forming obstacles to their propagation. During the compression strain application, partial back movement of twin dislocations, nucleation and propagation of new twinning systems compatible with the compression strain as well as glide of ordinary dislocations should be activated. These three kinds of movement are facilitated by the back stress created during the tensile strain, leading to the tension-compression asymmetry. As a result, a pronounced Bauschinger effect caused mainly by transient softening is observed during the compression part. In fact, if another test was performed by starting in compression first, we suspect that the asymmetry might change direction. When cycling at the same strain range, ordinary dislocations which are easily able to multiply and to accommodate both compression and tension strains propagate the applied deformation. The stress does not increase and therefore the twin network does not change drastically as twins thicken. Hence, the stabilized cycle is immediately reached. The same scenario occurs at high temperature. The bump is only less pronounced as deformation by ordinary disclocations is eased by the activation of cross slip.

The small cyclic hardening observed at room temperature is similar to the cyclic stress strain behavior that has been observed on an equiaxed

near-γ microstructure in [56], but different from the one observed on cast material for which a significant hardening was observed [13]. That hardening is usually associated to the formation of a vein-like dislocation structure and twin-dislocation interactions [5]. The mechanisms responsible for the absence of cyclic hardening at high temperature are unclear but are most certainly related to the capability of dislocations to cross-slip, promoting the dislocation annihilation processes, thus limiting the hardening.

The second type of behavior corresponds to microstructures with a high volume fraction of lamellar colonies. This behavior is characterized by a smooth entry to plasticity. The two investigated microstructures exhibit the same yield stresses but different 0.2 % yield stresses. This can be explain by the important plastic anisotropy of lamellar colonies that has been revealed by studying lamellar single colonies [57]. This anisotropy leads favorably oriented lamellar colonies to yield well before the macroscopic yield stress [58, 59]. Therefore when performing tests at the macroscopic scale, the grain size and lamellae size effects are only observed on the 0.2 % yield stresses following a Hall-Petch law. This is why in this work, from a macroscopic point of view, the microstructural attributes affect mostly the kinematic hardening and not the apparent yield stress.

During cyclic tests, a Bauschinger effect caused by transient softening is observed. The transient softening is far less pronounced than the one of microstructures with a high volume fraction of γ grains. Nevertheless, TEM observations suggest that the phenomena causing this softening are most certainly similar but less striking because of the multiscale aspect of lamellar microstructures [5]. As the deformation is constrained within lamellae, those

phenomena are not highlighted during macroscopic tests.

Regarding the strain rate sensitivity, multirate tensile test results show that the microstructure sensitivity to viscosity effects increases with the γ grain volume fraction. The relaxation parts of the tests reveal that the mechanical behavior upon very low strain rate is drastically modified by adding a small volume fraction of γ phase. Overall, it thus appears that the strain rate sensitivity is closely related to the microstructure γ phase volume fraction. This is an important observation as near-lamellar microstructures that consist of lamellar colonies with a fraction of globular γ grains are often considered as the optimal microstructure in TiAl alloys because of their balanced mechanical properties [28, 60].

5. Conclusions

The mechanical behavior of four generic TiAl microstructures has been studied at room and high temperature by means of mechanical testing, including cyclic plasticity experiments. The phenomena observed at the macroscopic scale are linked with their corresponding microscopic mechanisms. The mechanical behaviors can be classified in two categories.

Microstructures containing an important volume fraction of γ grains exhibit a pronounced Bauschinger effect caused mainly by a spectacular transient softening. This sudden softening is attributed to the onset of twinning and the dislocation-twin interactions. At room temperature, those microstructures exhibit a tension-compression asymmetry during cyclic tests that manifests as different elastic domain sizes depending on the flow stress direction.

Microstructure with a high volume fraction of lamellar colonies show little distinction between the elastic and plastic domains because of the multiscale aspect of the microstructure and the pronounced plastic anisotropy of lamellar colonies. A Bauschinger effect is also observed, partly caused by a transient softening that is far less significant than the one described above, but mostly due to a pronounced kinematic hardening. At the macroscopic scale, the impact of the lamellar microstructural attributes appears only on the kinematic hardening because of the multiscale aspect of the microstructure.

At 750 °C, the microstructure strength hierarchy and the observed phenomena are the same than those observed at room temperature. Particularly, the transient softening levels are almost exactly similar to the ones observed at room temperature. The strain rate sensitivity is shown to increase with the globular γ phase volume fraction. The relaxation parts of the tests revealed that even a low amount of globular γ grains deeply modifies the mechanical behavior upon very low strain rate.

To conclude, components made in TiAl alloys must be designed carefully as significant unwanted plasticity might occur upon strain reversal, particularly if the mechanical behavior is close to the one observed for the near-γ and duplex microstructures. The given experimental results open a fruitful opportunity for the microstructure-sensitive modeling of TiAl alloys mechanical behavior. Ongoing work focus on modeling the observed cyclic deformation by means of rate-dependent crystal plasticity and computational homogenization.

Aknowledgement

The authors would like to thank our colleagues Camille Liard for performing the experiments and Marc Thomas for providing the material and helpful discussions.

References

[1] BP Bewlay, S Nag, A Suzuki, and MJ Weimer. TiAl alloys in commercial aircraft engines. *Materials at High Temperatures*, 33(4-5):549–559, 2016.

[2] Young-Won Kim and Sang-Lan Kim. Advances in gammalloy materials–processes–application technology: successes, dilemmas, and future. *JOM*, 70(4):553–560, 2018.

[3] Jonathan DH Paul, Roland Hoppe, and Fritz Appel. On the Bauschinger effect in TiAl alloys. *Acta Materialia*, 104:101–108, 2016.

[4] T Nakano, HY Yasuda, N Higashitanaka, and Y Umakoshi. Anomalous behaviour of cyclic deformation and fatigue properties of TiAl PST crystals under constant applied stress. *Acta materialia*, 45(11):4807–4821, 1997.

[5] Anne-Lise Gloanec, Mustapha Jouiad, Denis Bertheau, Marjolaine Grange, and G Hénaff. Low-cycle fatigue and deformation substructures in an engineering TiAl alloy. *Intermetallics*, 15(4):520–531, 2007.

[6] Young-Won Kim and Dennis M Dimiduk. Progress in the understanding of gamma titanium aluminides. *JOM*, 43(8):40–47, 1991.

[7] Fritz Appel, Jonathan David Heaton Paul, and Michael Oehring. *Gamma titanium aluminide alloys: science and technology*. John Wiley & Sons, 2011.

[8] A Brotzu, F Felli, F Marra, D Pilone, and G Pulci. Mechanical properties of a TiAl-based alloy at room and high temperatures. *Materials Science and Technology*, 34(15):1847–1853, 2018.

[9] Hee Y Kim and Soon H Hong. Effect of microstructure on the high-temperature deformation behavior of Ti-48Al-2W intermetallic compounds. *Materials Science and Engineering: A*, 271(1-2):382–389, 1999.

[10] Ali El-Chaikh, Thomas K Heckel, and Hans-J Christ. Thermomechanical fatigue of titanium aluminides. *International Journal of Fatigue*, 53:26–32, 2013.

[11] Stephen-Peter Brookes, H-J Kühn, Birgit Skrotzki, Hellmuth Klingelhöffer, Rainer Sievert, J Pfetzing, D Peter, and G Eggeler. Axial–torsional thermomechanical fatigue of a near-γ TiAl-alloy. *Materials Science and Engineering: A*, 527(16-17):3829–3839, 2010.

[12] Fritz Appel, Thomas K Heckel, and Hans-Jürgen Christ. Electron microscope characterization of low cycle fatigue in a high-strength multiphase titanium aluminide alloy. *International Journal of Fatigue*, 32(5):792–798, 2010.

[13] Masahide Satoh, Susumu Horibe, Morihiko Nakamura, and Hiroyuki Uchida. Cyclic deformation and fatigue in TiAl intermetallic compound

under plastic strain control. *International Journal of Fatigue*, 32(4):698–702, 2010.

[14] O Berteaux, M Jouiad, M Thomas, and G Hénaff. Microstructure–low cycle fatigue behaviour relationships in a pm γ-TiAl alloy. *Intermetallics*, 14(10-11):1130–1135, 2006.

[15] G Malakondaiah and T Nicholas. High-temperature low-cycle fatigue of a gamma titanium aluminide alloy Ti-46Al-2Nb-2Cr. *Metallurgical and Materials Transactions A*, 27(8):2239, 1996.

[16] Gilbert Hénaff and Anne-Lise Gloanec. Fatigue properties of TiAl alloys. *Intermetallics*, 13(5):543–558, 2005.

[17] T Kruml and K Obrtlík. Microstructure degradation in high temperature fatigue of TiAl alloy. *International Journal of Fatigue*, 65:28–32, 2014.

[18] Benjamin Fournier, Maxime Sauzay, Christel Caës, Michel Noblecourt, and Michel Mottot. Analysis of the hysteresis loops of a martensitic steel: Part i: Study of the influence of strain amplitude and temperature under pure fatigue loadings using an enhanced stress partitioning method. *Materials Science and Engineering: A*, 437(2):183–196, 2006.

[19] David L McDowell. Microstructure-sensitive computational structure-property relations in materials design. In *Computational Materials System Design*, pages 1–25. Springer, 2018.

[20] BD Smith, DS Shih, and DL McDowell. Cyclic plasticity experiments and polycrystal plasticity modeling of three distinct ti alloy microstructures. *International Journal of Plasticity*, 101:1–23, 2018.

[21] F Coudon, S Gourdin, A Boucicaud, T Rose, and G Cailletaud. A stochastic approach applied to directionally solidified turbine blades. *International Journal of Solids and Structures*, 184:193–201, 2020.

[22] J-L Chaboche, Anais Gaubert, P Kanouté, Arnaud Longuet, Farida Azzouz, and Matthieu Mazière. Viscoplastic constitutive equations of combustion chamber materials including cyclic hardening and dynamic strain aging. *International journal of plasticity*, 46:1–22, 2013.

[23] M Grange, JL Raviart, and M Thomas. Influence of microstructure on tensile and creep properties of a new castable TiAl-based alloy. *Metallurgical and Materials Transactions A*, 35(7):2087–2102, 2004.

[24] Gerhard Wegmann, Rainer Gerling, and Frank-Peter Schimansky. Temperature induced porosity in hot isostatically pressed gamma titanium aluminide alloy powders. *Acta Materialia*, 51(3):741–752, 2003.

[25] Nikhilesh Chawla and X Deng. Microstructure and mechanical behavior of porous sintered steels. *Materials Science and Engineering: A*, 390(1-2):98–112, 2005.

[26] Caroline A Schneider, Wayne S Rasband, and Kevin W Eliceiri. Nih image to ImageJ: 25 years of image analysis. *Nature methods*, 9(7):671, 2012.

[27] Olivier Berteaux. *Etude des mécanismes d'écrouissage et d'endommagement cycliques des alliages TiAl élaborés par métallurgie des poudres*. PhD thesis, Poitiers, 2005.

[28] Thomas Voisin, Jean-Philippe Monchoux, Mickael Perrut, and Alain Couret. Obtaining of a fine near-lamellar microstructure in TiAl alloys by spark plasma sintering. *Intermetallics*, 71:88–97, 2016.

[29] H-J Christ, H Mughrabi, S Kraft, F Petry, R Zauter, and K Eckert. The use of plastic strain control in thermomechanical fatigue testing. In *Fatigue under thermal and mechanical loading: mechanisms, mechanics and modelling*, pages 1–14. Springer, 1996.

[30] Benjamin Fournier, Maxime Sauzay, Christel Caës, Michel Mottot, Michel Noblecourt, and André Pineau. Analysis of the hysteresis loops of a martensitic steel: Part ii: study of the influence of creep and stress relaxation holding times on cyclic behaviour. *Materials Science and Engineering: A*, 437(2):197–211, 2006.

[31] P Schallow and H-J Christ. High-temperature fatigue behaviour of a second generation near-γ titanium aluminide sheet material under isothermal and thermomechanical conditions. *International journal of fatigue*, 53:15–25, 2013.

[32] J Bauschinger. On the change of position of the elastic limit of iron and steel under cyclic variations of stress. *Mitt. Mech.-Tech. Lab., Munich*, 13(1), 1886.

[33] PB Pragnell, WM Stobbs, and PJ Withers. Considerations in the use of yield asymmetries for the analysis of internal stresses in metal matrix composites. *Materials Science and Engineering: A*, 159(1):51–63, 1992.

[34] PB Prangnell, T Downes, PJ Withers, and T Lorentzen. An examination of the mean stress contribution to the Bauschinger effect by neutron diffraction. *Materials Science and Engineering: A*, 197(2):215–221, 1995.

[35] LM Brown and WM Stobbs. The work-hardening of copper-silica v. equilibrium plastic relaxation by secondary dislocations. *Philosophical Magazine*, 34(3):351–372, 1976.

[36] Alan Howard Cottrell and DL Dexter. Dislocations and plastic flow in crystals. *American journal of physics*, 22:242–243, 1954.

[37] Doris Kuhlmann-Wilsdorf and Campbell Laird. Dislocation behavior in fatigue ii. friction stress and back stress as inferred from an analysis of hysteresis loops. *Materials Science and Engineering*, 37(2):111–120, 1979.

[38] X Feaugas and H Haddou. Grain-size effects on tensile behavior of nickel and AISI 316L stainless steel. *Metallurgical and materials transactions A*, 34(10):2329–2340, 2003.

[39] JI Dickson, J Boutin, and L Handfield. A comparison of two simple methods for measuring cyclic internal and effective stresses. *Materials Science and Engineering*, 64(1):L7–L11, 1984.

[40] Haifeng Xu, Duyi Ye, and Linbo Mei. A study of the back stress and the friction stress behaviors of Ti-6Al-4V alloy during low cycle fatigue at room temperature. *Materials Science and Engineering: A*, 700:530–539, 2017.

[41] H Haddou, M Risbet, G Marichal, and X Feaugas. The effects of grain size on the cyclic deformation behaviour of polycrystalline nickel. *Materials Science and Engineering: A*, 379(1-2):102–111, 2004.

[42] Shuai Dong, Qin Yu, Yanyao Jiang, Jie Dong, Fenghua Wang, Li Jin, and Wenjiang Ding. Characteristic cyclic plastic deformation in ZK60 magnesium alloy. *International Journal of Plasticity*, 91:25–47, 2017.

[43] Alain Couret, Guy Molénat, Jean Galy, and Marc Thomas. Microstructures and mechanical properties of TiAl alloys consolidated by spark plasma sintering. *Intermetallics*, 16(9):1134–1141, 2008.

[44] MR Kabir, Marion Bartsch, Liudmila Chernova, Klemens Kelm, and Janine Wischek. Correlations between microstructure and room temperature tensile behavior of a duplex TNB alloy for systematically heat treated samples. *Materials Science and Engineering: A*, 635:13–22, 2015.

[45] CT Liu and PJ Maziasz. Microstructural control and mechanical properties of dual-phase TiAl alloys. *Intermetallics*, 6(7-8):653–661, 1998.

[46] Alain Couret. Glide mechanism of ordinary dislocations in the γ phase of TiAl. *Intermetallics*, 9(10-11):899–906, 2001.

[47] H Jabbar, J-P Monchoux, M Thomas, and A Couret. Microstructures and deformation mechanisms of a G4 TiAl alloy produced by spark plasma sintering. *Acta Materialia*, 59(20):7574–7585, 2011.

[48] Jean-Philippe Monchoux, Jiangshan Luo, Thomas Voisin, and Alain Couret. Deformation modes and size effect in near-γ TiAl alloys. *Materials Science and Engineering: A*, 679:123–132, 2017.

[49] Florian Kauffmann, Thomas Bidlingmaier, Gerhard Dehm, Alexander Wanner, and Helmut Clemens. On the origin of acoustic emission during room temperature compressive deformation of a γ-TiAl based alloy. *Intermetallics*, 8(7):823–830, 2000.

[50] WT Marketz, FD Fischer, and H Clemens. Deformation mechanisms in TiAl intermetallics: experiments and modeling. *International Journal of Plasticity*, 19(3):281–321, 2003.

[51] S Farenc, A Coujou, and A Couret. An in situ study of twin propagation in TiAl. *Philosophical Magazine A*, 67(1):127–142, 1993.

[52] Premysl Beran, Milan Heczko, Tomas Kruml, Tobias Panzner, and Steven van Petegem. Complex investigation of deformation twinning in γ-TiAl by TEM and neutron diffraction. *Journal of the Mechanics and Physics of Solids*, 95:647–662, 2016.

[53] Slim Zghal and Alain Couret. Transmission of the deformation through γ-γ interfaces in a polysynthetically twinned TiAl alloy ii. twin interfaces (180 rotational). *Philosophical Magazine A*, 81(2):365–382, 2001.

[54] Haidong Fan, Sylvie Aubry, Athanasios Arsenlis, and Jaafar A El-Awady. The role of twinning deformation on the hardening response of polycrystalline magnesium from discrete dislocation dynamics simulations. *Acta Materialia*, 92:126–139, 2015.

[55] Ibrahim Karaman, Huseyin Sehitoglu, Yu I Chumlyakov, Hans J Maier, and IV Kireeva. The effect of twinning and slip on the bauschinger effect

of hadfield steel single crystals. *Metallurgical and Materials Transactions A*, 32(13):695–706, 2001.

[56] AL Gloanec, G Henaff, M Jouiad, D Bertheau, P Belaygue, and M Grange. Cyclic deformation mechanisms in a gamma titanium aluminide alloy at room temperature. *Scripta materialia*, 52(2):107–111, 2005.

[57] H Inui, MH Oh, A Nakamura, and M Yamaguchi. Room-temperature tensile deformation of polysynthetically twinned (PST) crystals of TiAl. *Acta Metallurgica et Materialia*, 40(11):3095–3104, 1992.

[58] Thomas Edward James Edwards, Fabio Di Gioacchino, Amy Jane Goodfellow, Gaurav Mohanty, Juri Wehrs, Johann Michler, and William John Clegg. Deformation of lamellar γ-TiAl below the general yield stress. *Acta Materialia*, 163:122–139, 2019.

[59] R Botten, Xinhua Wu, D Hu, and MH Loretto. The significance of acoustic emission during stressing of TiAl-based alloys. part i: Detection of cracking during loading up in tension. *Acta materialia*, 49(10):1687–1691, 2001.

[60] Helmut Clemens and Svea Mayer. Design, processing, microstructure, properties, and applications of advanced intermetallic TiAl alloys. *Advanced Engineering Materials*, 15(4):191–215, 2013.